Fibronectin acts as a molecular switch to determine SPARC function in pancreatic cancer.

Amanda Munasinghe[1], Khalisha Malik[1], Fatemia Mohamedi[1], Stan Moaraf[1,3], Hemant Kocher[2], Lucy Jones[1] and Natasha J Hill[1]*

[1] *Biomolecular Sciences Department, Kingston University, Kingston-upon-Thames, UK*
[2] *Centre for Tumour Biology, Barts Cancer Institute, Queen Mary University of London, London, UK.*

[3]*Current address: Department of Neurobiology, The I. Meier Segals Garden for Zoological Research, Tel Aviv University, Israel 6997801.*

*Corresponding author – Biomolecular Sciences Department, Kingston University, Penrhyn Road, Kingston-upon-Thames, KT1 2EE, UK. Tel: +44(0)2084172519. Email: n.hill@kingston.ac.uk

The authors declare that no competing interests exist.

ABSTRACT

Pancreatic ductal adenocarcinoma (PDAC) is one of the deadliest of all solid tumours and more effective therapy is urgently needed. The stroma is thought to play a critical role in tumour development and metastasis, and high stromal expression of the matricellular protein SPARC has been robustly associated with poor patient prognosis. However, the precise role of SPARC has been highly controversial, with multiple studies demonstrating tumour-suppressor properties of this protein *in vitro*. This conflicting data has been a barrier to the development of new therapeutic approaches targeting SPARC, despite current interest in stromal-therapy.

We show conclusively that SPARC acts directly on cancer cells to promote pancreatic cancer cell proliferation. This contradicts previous *in vitro* studies, but is consistent with the observed clinical association between SPARC expression and poor patient prognosis. However, depletion of fibronectin switches the activity of SPARC from promoting cancer cell proliferation to growth inhibition and induction of apoptosis. Thus, targeting the interaction between SPARC and fibronectin could be used to turn the highly expressed tumour protein SPARC against the tumour to induce tumour cytotoxicity, and is a novel target for PDAC therapy.

Keywords – matricellular, tumor stroma, apoptosis, extracellular matrix.

1. Introduction

Pancreatic ductal adenocarcinoma (PDAC) is a devastating disease, with one of the lowest survival rates of all cancers [1]. New therapeutic targets are urgently needed. One striking pathological feature of PDAC is the extent of the tumour stroma. The complex interaction between cancer cells, stromal cells and the extracellular matrix is thought to contribute to both tumour development and chemotherapy resistance. Activated pancreatic stellate cells are important drivers of the stromal response, causing an enhanced secretion of growth factors, cytokines and matrix proteins that supports cancer cell proliferation and metastasis [2]. SPARC is a stroma-derived protein that plays a critical role in this desmoplastic response [3]. High SPARC expression is strongly associated with poor patient prognosis in resectable and locally advanced pancreatic cancer [4–8]. Furthermore, it is clear that while SPARC is normally expressed at low levels in adult tissues, pancreatic tumours commonly express high levels of SPARC [9,10]. In line with this, serum SPARC level is being explored as a screening marker for pancreatic cancer [11].

The precise role of SPARC in tumour development and progression remains unclear. SPARC is a matricellular protein, capable of interacting with extracellular components such as matrix proteins and growth factors, as well as cell surface receptors such as integrins and growth factor receptors [12]. It is involved in varied cellular processes including proliferation, apoptosis, adhesion and migration, as well as matrix remodelling and angiogenesis [13]. However, despite the strong clinical association between SPARC over-expression and pancreatic cancer, published *in vitro* experiments to date conversely suggest that SPARC inhibits pancreatic cell proliferation and promotes apoptosis [9,14,15].

Our goal was to investigate this apparent contradiction using a range of *in vitro* models to examine the effect of SPARC in both stromal and cancer compartments. In doing so, we have discovered a novel therapeutic target for pancreatic cancer that allows us to 'switch' the highly tumour-expressed SPARC protein from promoting cancer cell growth to inducing pancreatic cancer cell apoptosis. This

may in the future allow us to turn the stroma against the cancer to more effectively treat this devastating disease.

2. Materials and Methods

2.1 Cell Culture

PS-1 cells were originally isolated from a donated human pancreas and immortalised as described previously [16]. PDAC cell lines AsPC-1, Panc-1, Hpaf and Capan-1 were kindly provided by Dr Charlotte Edling, formerly of the Blizard Institute, Barts and the London Queen Mary University of London. All cell lines were maintained in RPMI-1640 media supplemented with 10% FBS, 2mM L-glutamine, 100U/ml penicillin and 100µg/ml streptomycin purchased from Fisher Scientific, UK. Cells were incubated at 37°C in humidified air with 5% CO_2. All cell lines were sub-cultured every 3-4 days and used within 10 passages.

Additional proteins used for cell culture were as follows: rhSPARC (#941-SP-050, R&D Systems; His-tagged), active TGFβ1 (Abcam #ab50036), and fibronectin (#10042682, Fisher Scientific). Cell culture medium containing albumin was produced by substituting FBS with 2.5% BSA (Sigma-Aldrich, UK) which is equivalent to the amount of albumin in 10% FBS.

Cell culture medium containing FBS depleted of fibronectin (FN) was produced using Gelatin-Sepharose 4B (#17-0956-01, GE Healthcare), which binds to fibronectin with high specificity, adapted from the protocol described by Liu and Collodi [17]. Gelatin Sepharose 4B is supplied pre-swollen in 20% ethanol. The EtOH layer was removed by centrifugation and discarded. The beads were washed with PBS and 8ml was added to 50ml of FBS and the solutions were mixed on a lab tube roller mixer at 4˚C for 48hrs. Post-mixing, the FBS solution was centrifuged and the layer of fibronectin bound gelatin-sepharose 4B was discarded. This step was repeated once more and the resulting FBS was

filter sterilised (0.2µm). RPMI-1640 medium was supplemented with 10% FBS depleted of FN, 2mM L-glutamine, 100U/ml penicillin and 100µg/ml streptomycin.

2.2 Cell Proliferation Assay

AsPC-1, Capan-1, Hpaf-2, Panc-1 and PS-1 cells were plated at a density of $2x10^3$ or $4x10^3$ cells/well in a 96 well plate and treated with 0.5% FBS medium overnight. Cells were then treated +/- 10µg/ml rhSPARC, or with conditioned medium from siRNA transfected PS-1 cells, in the FBS conditions indicated. BrdU incorporation (Roche Applied Science) was measured for the last 24 hours of a 72 hour culture according to the manufacturer's instructions. Absorbance was read at 370nm on an Epoch Microplate Spectrophotometer (BioTek). In Figure 3A, $4x10^4$ PS-1 cells were seeded in a 24 well plate and transfected with SPARC or control siRNA. The cells were counted using a haemocytometer after a 48hr transfection period.

2.3 Transwell Model

AsPC-1 cells were plated at a density of $1.5x10^5$ cells/well in a 6 well insert companion plate (BD Biosciences) in complete medium. PS-1 cells previously transfected with either SPARC or control siRNA were introduced to the well using a 1µm porous insert (BD Biosciences). AsPC-1 cell number was counted using a haemocytometer for 5 consecutive days after the co-culture, or at day 6 with representative images captured using an IncuCyte Zoom Live cell imaging system.

2.4 siRNA Transfection

Transfection of PS-1 cells was carried out as described previously [18]. Briefly, transfection complexes were formed by mixing control- or SPARC-siRNA (Dharmacon, GEHealthcare) in HiPerFect transfection medium (Qiagen). During this period, PS-1 cells were cultured in a 24 well plate and subsequently treated with the transfection reagents to give a final siRNA concentration of 80nM, unless otherwise stated. The Dharmacon siRNA used were as follows: control non-targeting siRNA #J-001810-01; SPARC-targeting siRNA #J-003710-10 was used in all experiments except those shown in Figure 1E and Figure 5B, where an alternative SPARC-targeting siRNA #J-003710-09 was used. PS-1

cells were transfected for 48hrs and SPARC knockdown was confirmed by western blot (see Figure 1 for validation of siRNA knockdown).

2.5 PS-1 Cell Activation Assay/ Immunocytochemistry

All-trans retinoic acid (ATRA) has previously been shown to inactivate PS-1 cells [19]. ATRA (Sigma-Aldrich) was reconstituted in ethanol and stock ATRA solution was protected from light, stored at -80˚C and used within 2 weeks of reconstitution. Sterile #1.5 coverslips were placed in 6 well plates. PS-1 cells were seeded at density of $1x10^5$ cells/well in complete medium containing 1μM ATRA or vehicle control (Sigma-Aldrich). The plate was incubated for 7 days and the culture medium was replenished with fresh medium at day 3. At day 7, the cells were fixed with 4% PFA, blocked with 10% normal horse serum, incubated with an anti-GFAP antibody (Sigma-Aldrich) for 2hrs followed by a 1hr incubation with AlexaFluor488 secondary antibody. Slides were imaged using a 20x objective on a FLoid imaging station (Life Technologies). Cell lysates were also prepared at day 7 for western blot.

PS-1 cells transfected with either SPARC or control siRNA were plated on coverslips in a 6 well plate at a density of $1x10^5$ cells/ml in low serum (0.5% FBS) or complete medium (10% FBS) for 72hrs. Cells were fixed with 10% NBF, permeabilised with 0.1% Triton-X, blocked with 10% NHS, incubated with an anti-vimentin primary antibody (Dako) for 2hrs and an Alexafluor488 secondary antibody (Life Technologies) for 1hr. Slides were imaged at 10x lens on a EVOS microscope (AMG). See Supplementary Table 1 for antibody details.

2.6 Collagen I immunocytochemistry

SPARC/control siRNA transfected PS-1 cells were re-plated into a 6-well plate containing sterilized coverslips and cultured for 72hrs. Post culture, the cells were washed in PBS and fixed with 4% PFA for 10 min at RT, washed again and blocked in 10% normal horse serum for 30 min at RT. The cells were incubated overnight at 4˚C with anti-collagen I antibody (#ab19811, Abcam), then washed and incubated with an Alexafluor 488 secondary (#A-11055, Invitrogen) for 1hr at RT. The cells were then

incubated with DAPI (1:1000 dilution, #D3571, Invitrogen) for 5min at RT. The cells were washed and mounted onto slides and imaged with a Zeiss LSM confocal microscope.

2.7 Western Blot

Cells lysates were made with RIPA lysis buffer containing Halt protease inhibitor cocktail (Thermo Scientific). Lysate supernatant was collected after centrifugation. Protein was quantified using a BCA assay (Bio-Rad) before loading according to manufacturer's instructions, and an anti-β actin antibody was used as a loading control. The lanes have been re-ordered for clarity in some blots.

For glycosylase experiments, PNGase F was incubated with the lysates for 1hr at 37˚C post denaturation at 100˚C according to manufacturer's protocol (New England Biosciences).

After the addition of 5X sample buffer, proteins were resolved using handmade 12% SDS-PAGE gels, transferred onto a nitrocellulose membrane using semi-dry transfer, and blocked with 5% semi-skimmed milk in TTBS. The membranes were incubated overnight at 4˚C with relevant primary antibodies against SPARC, TGF-β or vimentin and β-actin. Goat anti-rabbit and anti-mouse IgG secondary antibodies conjugated to IR700 and IR800 infra-red dyes were used for detection and the Odyssey CLx Infrared Imaging System (Li-Cor) was used for visualisation. Band molecular weight and intensity quantification was measured using Li-Cor Image Studio Lit version 4.0. See Supplementary Table 1 for antibody details.

The blots for collagen and αSMA were performed similarly but with the following differences. 10µg of protein were loaded per lane on a 4–20% Mini-PROTEAN TGX Precast Protein Gels (#4561093, Bio-Rad). A Tansblot Turbo Transfer System (Bio-Rad) was used to transfer proteins onto a 0.2µm nitrocellulose membrane. A Trans-Blot Turbo RTA Mini Nitrocellulose Transfer Kit (#1704270, Bio-Rad) was used according to manufacturer's instruction. Membranes were incubated with primary antibodies against collagen I (ab34710, Abcam) and α-SMA (ab7817, Abcam) rocking overnight at 4˚C.

2.8 ELISA

For SPARC secretion, an RnD Systems Human SPARC Quantikine ELISA Kit (#DSP00) was used. Conditioned medium from SPARC/control siRNA transfected PS-1 cells (in 0.5% FBS) was collected and diluted 8-fold in Calibrator Diluent RD6-59. To quantify fibronectin, a bovine Fibronectin ELISA Kit (Sigma #RAB1011-1KT) was used, which also recognises human fibronectin. Samples of FBS and FBS depleted of FN were diluted 500-fold in Assay/Sample Diluent buffer, or for PS-1-conditioned media samples were diluted 50-fold. Standards were prepared and the protocol was carried out according to the manufacturer's instructions for both kits. Absorbance was read at 450nm using a FLUORstar microplate reader (BMG Labtech).

2.9 Caspase-3/7 apoptosis assay

Cancer cells were seeded at a density of 4,000 cells/well in a 96 well plate in low serum medium overnight to synchronize. The cells were treated with 10µg/ml rhSPARC, or left untreated, in complete or low serum medium supplemented with 5µm unlabelled caspase -3/-7 substrate (DEVD) that releases a green DNA binding fluorescent label upon caspase cleavage (Essen Bioscience). Apoptotic cells therefore fluoresce. An IncuCyte Zoom Live Cell Imaging System was used to capture phase contrast and green fluorescence images over 72hrs. The IncuCyte Zoom 2015A software was used to calculate the stained apoptotic cell area in the images.

2.10 Annexin V apoptosis assay

AsPC-1 cells were seeded at a density of 50,000 cells/well in a 12-well plate overnight in low serum (0.5% FBS) medium to synchronize the cells. The cells were subsequently treated with or without 10µg/ml rhSPARC in complete or FN depleted medium and cultured for 72hrs. Post culture, the cells were resuspended in medium and 10µl was removed for cell counting using a hemocytometer. The remaining cell suspension was washed with PBS and resuspended in a 100µl of 1X Annexin binding buffer (#556454, BD Bioscience) diluted in cold PBS. Samples were incubated with 5µl FITC Annexin V (#560931, BD Bioscience) and 5µl 7AAD (#559925, BD Bioscience) and incubated for 15min at RT in

the dark. A further 400µl of 1X binding buffer was added to each sample before being analysed immediately using a flow cytometer (BD Bioscience).

2.11 Statistics

Statistical significance was measured using unpaired two-tailed Student's T-test unless indicated as a two-way ANOVA. A p value of ≤0.05 was considered statistically significant. Error bars represent standard error of the mean (SEM).

3. Results

3.1 Stromal cell secreted SPARC promotes pancreatic cancer cell growth.

SPARC is primarily expressed by stromal cells in both PDAC tumours and cell lines [5,14,15]. Consistent with this, SPARC was detectable at high levels in pancreatic stellate (PS-1) cells in our hands by western blot [20], and was undetectable in pancreatic cancer cells (Figure 1A). In order to examine the effect of stromal-derived SPARC on pancreatic cancer cell proliferation, we treated PS-1 cells with either control- or SPARC-siRNA, typically achieving ~85% knockdown (Figure 1B-E). SPARC siRNA treatment also reduced SPARC secretion by ~75%, as determined by ELISA (Figure 1F). Conditioned media from these PS-1 cells was then used to culture pancreatic cancer cells. As shown in Figure 2A, the proliferation of cancer cells cultured in SPARC-knockdown PS-1 cell medium was significantly reduced compared to cancer cells cultured in medium from control PS-1 cells. Pancreatic cancer proliferation was also found to be reduced by around 50% in the absence of PS-1-derived SPARC in experiments using a transwell model, as determined both by manual counting and quantitative imaging (Figure 2B&C). Together, these experiments show that PS-1-derived SPARC promotes pancreatic cancer proliferation, in direct contrast to previously reported studies [14,15], but consistent with clinical observations linking high SPARC expression with poor patient prognosis [4–8].

3.2 SPARC protein expression is upregulated in activated pancreatic stellate cells but does not exhibit cell autonomous action.

To try to identify the reason behind the difference between our results and those previously reported, we hypothesized that PS-1-derived SPARC may act in a cell autonomous manner to promote PS-1 cell activation and the production of secreted factors, thereby indirectly promoting pancreatic cancer cell proliferation. We therefore conducted a series of experiments to examine whether SPARC siRNA knockdown affects the activation of PS-1 cells. Activated PS-1 cells are known to have increased proliferation and increased expression of the cytoskeletal protein vimentin compared to quiescent cells [19]. However, there was no evidence of any difference in PS-1 proliferation either directly following SPARC siRNA knockdown, as determined by manual cell counting (Figure 3A) and quantitative Image J analysis (Figure 3G), or following re-plating and culture in conditioned media, as determined by BrdU assay (Figure 3B). Similarly, treatment with recombinant SPARC did not affect PS-1 cell proliferation (Figure 3C). Western blot and immunocytochemistry staining for vimentin in PS-1 cells following transfection with control- or SPARC-siRNA showed no change in vimentin expression (Figure 3D-F). Expression of the important cancer growth factor TGF-β also remained unchanged in SPARC-siRNA transfected PS-1 cells over 3 days (Figure 3H&I). Furthermore, no significant change in the expression of collagen I was observed by quantitative confocal microscopy (Suppl. Figure 2F-H), although a slight increase in collagen I was detected in SPARC knockdown cells by Western blot (Suppl. Figure 2I), consistent with previous reports [21]. No difference in fibronectin secretion was observed, as determined by ELISA (Suppl. Figure 3B). Similarly, no clear difference in expression of the myofibroblast activation marker α-SMA, which has been associated with a tumour-suppressive subset of myofibroblasts [22], was observed (Suppl. Figure 2J). Taken together, this data shows that no difference in PS-1 activation was detected following SPARC siRNA knockdown. We were therefore unable to find any evidence of SPARC playing a cell autonomous role, suggesting instead that SPARC secreted by PS-1 cells acts directly on pancreatic cancer cells to enhance their proliferation.

Interestingly, however, SPARC expression was significantly higher in activated PS-1 cells compared to quiescent cells (Suppl. Figure 1). We used all-trans retinoic acid (ATRA) to induce quiescence in PS-1 cells [19], and observed the expected increase in expression of the quiescence marker glial fibrillary acidic protein (GFAP), as well as a decrease in cell density, reflective of decreased proliferation following ATRA treatment. The increased expression of SPARC in activated pancreatic stellate cells is consistent with the clinically observed enhanced production of SPARC by aberrantly activated stromal cells in PDAC.

3.3 Purified SPARC recapitulates the effect of PS-1-derived SPARC in promoting pancreatic cancer cell growth.

In the absence of evidence that SPARC affects PS-1 activation in a cell autonomous manner, we therefore focused on mechanisms in which SPARC acts directly on pancreatic cancer cells. We hypothesized that purified SPARC, as used in previous studies [9,14,15], may be distinct to stromal-derived SPARC. SPARC is known to be glycosylated [23] and tissue-specific glycosylation patterns, or indeed tissue-specific isoform expression, could influence SPARC function. However, there was no evidence of any difference in molecular weight between rhSPARC and PS-1-derived SPARC over and above the expected slightly higher molecular weight of rhSPARC due to the presence of the His-tag (Figure 4A&B). Following removal of N-linked glycosylation by PNGase treatment, a mean shift in molecular weight of 3.1 kDa and 2.6 kDa was seen in rhSPARC and PS-1-derived SPARC, respectively, confirming glycosylation of both forms of SPARC, and potentially slightly increased glycosylation of the recombinant form compared to stromal SPARC. However, surprisingly, treatment with rhSPARC at a concentration similar to published studies [9,14,15] increased the proliferation of pancreatic cancer cells in our hands (Figure 4C), entirely consistent with the effect of stromal SPARC (Figure 2). Therefore potential differences in post-translational modification or cell-type specific isoform expression do not explain the contradiction between our observations and that in the literature of the effect of SPARC on pancreatic cancer cell proliferation.

3.4 Fibronectin switches SPARC activity from promoting pancreatic cancer cell growth to inducing cancer cell apoptosis.

Many of the published *in vitro* studies of SPARC were conducted under low or unspecified serum conditions [9,14,15], while we had used standard 10% serum in our assays. We therefore tested whether performing our experiments in low serum conditions affected the outcome. Culture of pancreatic cancer cells in low serum (0.5% FBS) conditioned medium from PS-1 cells transfected with control- or SPARC-siRNA showed, strikingly, that SPARC inhibits pancreatic cancer cell proliferation under low serum conditions (Figure 5A). This is in direct contrast to our previous observations in complete medium (Figure 2 and Figure 4C). The results were confirmed using a second siRNA targeting a distinct SPARC sequence, clearly demonstrating that the contrasting effects of SPARC are determined by serum conditions (Figure 5B). Experiments to test for cell autonomous functions of SPARC in PS-1 cells under low serum conditions showed that neither rhSPARC nor PS-1 derived SPARC has any effect on PS-1 cell proliferation or TGF-β expression (Supplementary Figure 2), consistent with observations in complete medium (Figure 3), suggesting that SPARC also acts directly on pancreatic cancer cells under low serum conditions.

We then performed a systematic *in silico* analysis of proteins for which there is evidence for interaction with SPARC and that are present in serum and may therefore be responsible for the switch between pro- and anti-proliferative SPARC function under different serum conditions (Supplementary Table 2). Although not exhaustive, the analysis revealed that of the 24 proteins for which there is evidence of interaction with SPARC in either the STRING or Gene/NCBI databases, 10 of these are typically present in serum, including albumin, TGF-β and fibronectin.

SPARC was originally identified as albumin-binding protein and albumin constitutes approximately half the total protein in plasma [24–26]. We therefore tested whether adding albumin into low serum cultures was able to 'switch' the effect of SPARC on pancreatic cancer cell proliferation. AsPC-1 cells were cultured with medium supplemented with 10% FBS, 0% FBS or 0.25% BSA (equivalent to

the BSA found in FBS) in the presence or absence of rhSPARC. As shown in Figure 5C, rhSPARC promoted AsPC-1 proliferation in complete medium and inhibited growth in serum free medium, as expected. However, SPARC also inhibited cell growth in the presence of BSA added to serum-free medium, suggesting that albumin does not affect the 'switch' in SPARC function caused by serum conditions.

SPARC has been shown to regulate signalling downstream of TGF-β, which is an important tumour growth factor, and it has been shown experimentally that SPARC can interact with the TGF-β/type II receptor complex [27,28]. To determine the effect of TGF-β on SPARC function, AsPC-1 cells in low serum medium (0.5% FBS) were treated with 10μg/ml rhSPARC, 140 ng/ml rhTGF-β, or both rhSPARC and TGF-β. As expected, SPARC treatment alone inhibited AsPC-1 proliferation, while TGF-β treatment alone had no significant effect (Figure 5D). However, TGF-β actually enhanced SPARC's ability to inhibit pancreatic cancer cell proliferation under low serum conditions compared to treatment with SPARC alone. Therefore, since TGF-β did not reverse SPARC-induced growth inhibition under low serum conditions, TGF-β was excluded as the serum factor that regulates SPARC function.

Fibronectin is also part of the SPARC interaction network (Suppl. Table 2), and is overexpressed in multiple tumours, including PDAC, as part of the desmoplastic reaction [29]. While fibronectin can be secreted locally by cells within tissues (cFN) it is also an abundant soluble plasma protein (pFN) [30]. Fibronectin can be depleted from serum using the well-established method of gelatin-sepharose columns [31,32], and effective fibronectin depletion was achieved in our hands using this approach as determined by ELISA quantification of fibronectin before and after depletion (Suppl. Figure 3A). We therefore tested whether depletion of pFN is able to 'switch' the SPARC effect. Consistent with previous experiments, SPARC promoted growth of AsPC-1 cells in 10% FBS and inhibited proliferation in low serum medium. However, strikingly, when AsPC-1 cells were treated with rhSPARC in complete medium depleted of fibronectin, the proliferative effect of SPARC

observed in 10% FBS medium was lost (Figure 5E). Instead, SPARC inhibited proliferation, mimicking the SPARC response in 0.5% FBS medium. This suggests that the presence of pFN in serum is responsible for 'switching' the effect of SPARC, such that in the presence of pFN SPARC promotes cell growth, while in conditions of low pFN SPARC inhibits cell growth.

While fibronectin depletion using gelatin-sepharose beads is highly specific, a small number of other gelatin-binding serum proteins can also be depleted using this technique, specifically MMP-2 and MMP-9 [33], as well as glycosaminoglycans such as heparin [34,35]. We therefore purchased purified bovine fibronectin in order to add fibronectin to low serum cultures to test whether the addition of purified fibronectin mimics the presence of 10% FBS and 'switches' the SPARC response. Additional of either 500μg/ml or 1 mg/ml fibronectin was sufficient to prevent the inhibition of cell proliferation induced by SPARC under low serum conditions (Figure 5F&G). Interestingly, SPARC did not cause increased proliferation when fibronectin was added, potentially due to the removal of heparin sulphate proteoglycans, which are known to be important for fibronectin function, during fibronectin purification. In summary, this data confirms that the presence of fibronectin controls SPARC activity.

In order to test whether SPARC is able to actively induce cytotoxicity under low serum/low fibronectin conditions, we measured activity of caspase-3/7 following SPARC treatment under both low and standard serum conditions. As shown in Figure 6A-C, in low serum conditions SPARC induces Caspase-3/7-activity, while in the presence of 10% serum SPARC inhibits Caspase-3/7 activity. Furthermore, treatment with SPARC in fibronectin-depleted 10% serum reduced cell number and increased apoptosis by ~50%, as shown by increased binding of Annexin-V (Figure 6D-F). Together, these data strongly suggest that inhibiting the interaction between SPARC and fibronectin would not only prevent SPARC from enhancing tumour growth, but would turn this highly expressed tumour stroma protein against the cancer cells to induce pancreatic cancer cell cytotoxicity.

4. Discussion

Conflicting evidence for the pro-/anti-proliferative effects of SPARC in different contexts has been a barrier to the development of therapeutic strategies relating to SPARC, despite clinical evidence demonstrating the association between high stromal SPARC expression and poor patient outcome in multiple tumour types, including pancreatic cancer [4,36]. *In vivo* experiments have provided useful insights, but since studies to date have used a systemic SPARC knockout approach, rather than cell-type specific, and since the lack of SPARC during development results in profound matrix abnormalities that are unlikely to reflect clinical pancreatic cancer, where SPARC is locally upregulated, the results overall have been challenging to interpret [37–43]. The interpretation of *in vitro* studies has been confounded by the wide array of different experimental scenarios, for example, knockdown/overexpression of endogenous SPARC in cancer cells *versus* modulation of SPARC in stromal cells or treatment of cancer cells with exogenous SPARC. There is evidence that SPARC may function intracellularly in cancer cells [44], and it has been shown that cancer cells expressing SPARC secrete very little or no SPARC [14,15]. Therefore, modulation of SPARC expression endogenously within cancer cells is likely to have distinct effects to those of extracellular SPARC. Further adding to this complexity, protocols involving an array of different serum and stress conditions are also employed. One conclusion that can be drawn from the confusing diversity of *in vitro* findings is that 'context' is important and influences the effect that SPARC has on cellular function. However, to date, no specific molecular basis for the hypothesized contextual factors that regulate SPARC function has been found. On re-examining the literature, a number of early studies in other models also found indications that serum and matrix conditions can regulate SPARC function [45,46]. However, our data show specifically for the first time that the presence of plasma fibronectin determines the specific effect of SPARC on pancreatic cancer cell proliferation, supporting the idea that precise extracellular matrix composition is the 'context' that determines SPARC function, potentially via modulation of integrin signalling [40,47] SPARC can enhance fibronectin matrix deposition *via* an integrin-linked kinase (ILK)-dependent mechanism [48,49], and in the absence of SPARC, fibronectin-induced actin filament rearrangement is inhibited [48]. It will

therefore be important in future studies to establish whether SPARC regulation of fibronectin is relevant to the 'switch' in SPARC function that we have observed in the absence of fibronectin.

The data shown here creates the exciting possibility that targeting interactions between specific matrix/matricellular proteins can be used to "fine-tune" the stroma, and represents a novel therapeutic approach for the treatment of solid tumours, particularly where there is a strong stromal component. Both SPARC and fibronectin are overexpressed in the PDAC tumour stroma, and targeting the interaction between SPARC and fibronectin could potentially turn the highly tumour expressed protein SPARC against the tumour, such that instead of promoting tumour growth it instead induces tumour cytotoxicity. The extracellular nature of this interaction makes it an attractive therapeutic target, with the additional potential advantage that intracellular SPARC functions would be left intact. There is clinical heterogeneity in terms of SPARC expression, and any future therapeutics targeting the SPARC-fibronectin interaction would likely benefit the ~2/3 of PDAC patients in which SPARC expression is upregulated in the stromal compartment [4].

In conclusion, we have shown that fibronectin acts as a molecular switch, controlling whether SPARC promotes pancreatic cancer cell proliferation or induces cancer cell cytotoxicity. It will be important to determine whether blocking this interaction, perhaps using either existing or novel antibodies, can be used therapeutically to turn the stroma against the tumour to more effectively treat pancreatic cancer. This novel approach may also have potential benefit in other types of solid tumour.

Acknowledgements.

The authors would like to thank Prof Tony Walker and Dr Charlotte Edling for useful discussions.

Author contributions.

AD performed the majority of experiments, analysed and presented the data, and co-wrote the manuscript. NH conceived and led the project, was involved in the analysis and presentation of data, and co-wrote the manuscript. KM contributed to additional experiments in Figures 1 and 5, and Suppl. Figures 2 & 3. FM contributed the data in Supplementary Figure 1(A-C), SM contributed to data in Figure 2B. LJ contributed to the development of the project. HK contributed to the editing of the manuscript. The corresponding author (NH) confirms she has had full access to the data in the study and final responsibility for the decision to submit for publication.

Funding.

This work was supported by Kingston University.

References.

[1] P. Rawla, T. Sunkara, V. Gaduputi, Epidemiology of Pancreatic Cancer: Global Trends, Etiology and Risk Factors, World J. Oncol. 10 (2019) 10–27. https://doi.org/10.14740/wjon1166.

[2] R. Kadaba, H. Birke, J. Wang, S. Hooper, C.D. Andl, F. Di Maggio, E. Soylu, M. Ghallab, D. Bor, F.E. Froeling, S. Bhattacharya, A.K. Rustgi, E. Sahai, C. Chelala, P. Sasieni, H.M. Kocher, Imbalance of desmoplastic stromal cell numbers drives aggressive cancer processes., J. Pathol. 230 (2013) 107–17. https://doi.org/10.1002/path.4172.

[3] H.Y. Tanaka, K. Kitahara, N. Sasaki, N. Nakao, K. Sato, H. Narita, H. Shimoda, M. Matsusaki, H. Nishihara, A. Masamune, M.R. Kano, Pancreatic stellate cells derived from human pancreatic cancer demonstrate aberrant SPARC-dependent ECM remodeling in 3D engineered fibrotic tissue of clinically relevant thickness, Biomaterials. 192 (2019) 355–367. https://doi.org/10.1016/j.biomaterials.2018.11.023.

[4] J.R. Infante, H. Matsubayashi, N. Sato, J. Tonascia, A.P. Klein, T.A. Riall, C. Yeo, C. Iacobuzio-Donahue, M. Goggins, Peritumoral fibroblast SPARC expression and patient outcome with resectable pancreatic adenocarcinoma, J. Clin. Oncol. 25 (2007) 319–325. https://doi.org/10.1200/JCO.2006.07.8824.

[5] T.S. Mantoni, R.R.E. Schendel, F. Rödel, G. Niedobitek, O. Al-Assar, A. Masamune, T.B. Brunner, Stromal SPARC expression and patient survival after chemoradiation for non-resectable pancreatic adenocarcinoma, Cancer Biol. Ther. 7 (2008) 1807–1816. https://doi.org/10.4161/cbt.7.11.6846.

[6] M. Sinn, B. V. Sinn, J.K. Striefler, J.L. Lindner, J.M. Stieler, P. Lohneis, S. Bischoff, H. Bläker, U. Pelzer, M. Bahra, M. Dietel, B. Dörken, H. Oettle, H. Riess, C. Denkert, SPARC expression in resected pancreatic cancer patients treated with gemcitabine: results from the CONKO-001 study, Ann. Oncol. 25 (2014) 1025–1032. https://doi.org/10.1093/annonc/mdu084.

[7] R. Shintakuya, N. Kondo, Y. Murakami, K. Uemura, N. Nakagawa, K. Okano, S. Takahashi, T. Sueda, The high stromal SPARC expression is independently associated with poor survival of patients with resected pancreatic ductal adenocarcinoma treated with adjuvant gemcitabine

in combination with S-1 or adjuvant gemcitabine alone, Pancreatology. 18 (2018) 191–197. https://doi.org/10.1016/j.pan.2017.12.014.

[8] J. Vaz, D. Ansari, A. Sasor, R. Andersson, SPARC: A potential prognostic and therapeutic target in pancreatic cancer, Pancreas. 44 (2015) 1024–1035. https://doi.org/10.1097/MPA.0000000000000409.

[9] A. Guweidhi, J. Kleeff, H. Adwan, N.A. Giese, M.N. Wente, T. Giese, M.W. Büchler, M.R. Berger, H. Friess, Osteonectin influences growth and invasion of pancreatic cancer cells, Ann. Surg. 242 (2005) 224–234. https://doi.org/10.1097/01.sla.0000171866.45848.68.

[10] C. Gundewar, A. Sasor, K.S. Hilmersson, R. Andersson, D. Ansari, The role of SPARC expression in pancreatic cancer progression and patient survival, Scand. J. Gastroenterol. 50 (2015) 1170–1174. https://doi.org/10.3109/00365521.2015.1024281.

[11] A. Papapanagiotou, G. Sgourakis, K. Karkoulias, D. Raptis, E. Parkin, P. Brotzakis, S. Panchal, A.G. Papavassiliou, Osteonectin as a screening marker for pancreatic cancer: A prospective study, J. Int. Med. Res. 46 (2018) 2769–2779. https://doi.org/10.1177/0300060518772413.

[12] J.E. Murphy-Ullrich, E.H. Sage, Revisiting the matricellular concept, Matrix Biol. 37 (2014) 1–14. https://doi.org/10.1016/j.matbio.2014.07.005.

[13] A.D. Bradshaw, E.H. Sage, SPARC, a matricellular protein that functions in cellular differentiation and tissue response to injury, J. Clin. Invest. 107 (2001) 1049–1054. https://doi.org/10.1172/JCI12939.

[14] N. Sato, N. Fukushima, N. Maehara, H. Matsubayashi, J. Koopmann, G.H. Su, R.H. Hruban, M. Goggins, SPARC/osteonectin is a frequent target for aberrant methylation in pancreatic adenocarcinoma and a mediator of tumor-stromal interactions, Oncogene. 22 (2003) 5021–5030. https://doi.org/10.1038/sj.onc.1206807.

[15] G. Chen, X. Tian, Z. Liu, S. Zhou, B. Schmidt, D. Henne-Bruns, M. Bachem, M. Kornmann, Inhibition of endogenous SPARC enhances pancreatic cancer cell growth: Modulation by FGFR1-III isoform expression, Br. J. Cancer. 102 (2010) 188–195. https://doi.org/10.1038/sj.bjc.6605440.

[16] F.E.M. Froeling, T.A. Mirza, R.M. Feakins, A. Seedhar, G. Elia, I.R. Hart, H.M. Kocher, Organotypic culture model of pancreatic cancer demonstrates that stromal cells modulate E-cadherin, β-catenin, and ezrin expression in tumor cells, Am. J. Pathol. 175 (2009) 636–648. https://doi.org/10.2353/ajpath.2009.090131.

[17] X. Liu, P. Collodi, Novel Form of Fibronectin from Zebrafish Mediates Infectious Hematopoietic Necrosis Virus Infection, J. Virol. 76 (2002) 492–498. https://doi.org/10.1128/jvi.76.2.492-498.2002.

[18] K. Viloria, A. Munasinghe, S. Asher, R. Bogyere, L. Jones, N.J. Hill, A holistic approach to dissecting SPARC family protein complexity reveals FSTL-1 as an inhibitor of pancreatic cancer cell growth, Sci. Rep. 6 (2016) 1–19. https://doi.org/10.1038/srep37839.

[19] F.E.M. Froeling, C. Feig, C. Chelala, R. Dobson, C.E. Mein, D.A. Tuveson, H. Clevers, I.R. Hart, H.M. Kocher, Retinoic acid-induced pancreatic stellate cell quiescence reduces paracrine Wntβ-catenin signaling to slow tumor progression, Gastroenterology. 141 (2011) 1486-1497.e14. https://doi.org/10.1053/j.gastro.2011.06.047.

[20] C.L. Ryall, K. Viloria, F. Lhaf, A.J. Walker, A. King, P. Jones, D. Mackintosh, R. McNeice, H.

Kocher, M. Flodstrom-Tullberg, C. Edling, N.J. Hill, Novel role for matricellular proteins in the regulation of islet βcell survival: The effect of SPARC on survival, proliferation, and signaling, J. Biol. Chem. 289 (2014) 30614–30624. https://doi.org/10.1074/jbc.M114.573980.

[21] B.S. Harris, Y. Zhang, L. Card, L.B. Rivera, R.A. Brekken, A.D. Bradshaw, SPARC regulates collagen interaction with cardiac fibroblast cell surfaces, Am. J. Physiol. - Hear. Circ. Physiol. 301 (2011). https://doi.org/10.1152/ajpheart.01247.2010.

[22] A. Neesse, C.A. Bauer, D. Öhlund, M. Lauth, M. Buchholz, P. Michl, D.A. Tuveson, T.M. Gress, Stromal biology and therapy in pancreatic cancer: Ready for clinical translation?, Gut. 68 (2019) 159–171. https://doi.org/10.1136/gutjnl-2018-316451.

[23] B. Kaufmann, S. Müller, F.G. Hanisch, U. Hartmann, M. Paulsson, P. Maurer, F. Zaucke, Structural variability of BM-40/SPARC/osteonectin glycosylation: Implications for collagen affinity, Glycobiology. 14 (2004) 609–619. https://doi.org/10.1093/glycob/cwh063.

[24] E.H. Sage, C. Johnson, P. Bornstein, Characterization of a novel serum albumin-binding glycoprotein secreted by endothelial cells in culture., J. Biol. Chem. 259 (1984) 3993–4007. https://www.ncbi.nlm.nih.gov/pubmed/6368555 (accessed December 3, 2019).

[25] H. Sage, R.B. Vernon, S.E. Funk, E.A. Everitt, J. Angello, SPARC, a secreted protein associated with cellular proliferation, inhibits cell spreading in vitro and exhibits Ca+2-dependent binding to the extracellular matrix, J. Cell Biol. 109 (1989) 341–356. https://doi.org/10.1083/jcb.109.1.341.

[26] A. Farrugia, Albumin Usage in Clinical Medicine: Tradition or Therapeutic?, Transfus. Med. Rev. 24 (2010) 53–63. https://doi.org/10.1016/j.tmrv.2009.09.005.

[27] A. Francki, T.D. McClure, R.A. Brekken, K. Motamed, C. Murri, T. Wang, E.H. Sage, SPARC regulates TGF-beta1-dependent signaling in primary glomerular mesangial cells, J. Cell. Biochem. 91 (2004) 915–925. https://doi.org/10.1002/jcb.20008.

[28] L.B. Rivera, R.A. Brekken, SPARC promotes pericyte recruitment via inhibition of endoglin-dependent TGF-β1 activity, J. Cell Biol. 193 (2011) 1305–1319. https://doi.org/10.1083/jcb.201011143.

[29] M. Korc, Pancreatic cancer-associated stroma production, Am. J. Surg. 194 (2007). https://doi.org/10.1016/j.amjsurg.2007.05.004.

[30] W.S. To, K.S. Midwood, Plasma and cellular fibronectin: Distinct and independent functions during tissue repair, Fibrogenes. Tissue Repair. 4 (2011). https://doi.org/10.1186/1755-1536-4-21.

[31] E. Ruoslahti, E.G. Hayman, M. Pierschbacher, E. Engvall, Fibronectin: Purification, Immunochemical Properties, and Biological Activities, Methods Enzymol. 82 (1982) 803–831. https://doi.org/10.1016/0076-6879(82)82103-4.

[32] S.I. Miekka, K.C. Ingham, D. Menache, Rapid methods for isolation of human plasma fibronectin, Thromb. Res. 27 (1982) 1–14. https://doi.org/10.1016/0049-3848(82)90272-9.

[33] S. Pal, Z. Chen, X. Xu, M. Mikhailova, B. Steffensen, Co-purified gelatinases alter the stability and biological activities of human plasma fibronectin preparations, J. Periodontal Res. 45 (2010) 292–295. https://doi.org/10.1111/j.1600-0765.2009.01241.x.

[34] E. Ruoslahti, E. Engvall, Complexing of fibronectin glycosaminoglycans and collagen., Biochim.

Biophys. Acta. 631 (1980) 350–8. https://doi.org/10.1016/0304-4165(80)90308-6.

[35] S.C. Stamatoglou, J.M. Keller, Interactions of cellular glycosaminoglycans with plasma fibronectin and collagen., Biochim. Biophys. Acta. 719 (1982) 90–7. https://doi.org/10.1016/0304-4165(82)90311-7.

[36] A.J. Sawyer, T.R. Kyriakides, Matricellular proteins in drug delivery: Therapeutic targets, active agents, and therapeutic localization, Adv. Drug Deliv. Rev. 97 (2016) 56–68. https://doi.org/10.1016/j.addr.2015.12.016.

[37] P.A. Puolakkainen, R.A. Brekken, S. Muneer, E.H. Sage, Enhanced growth of pancreatic tumors in SPARC-null mice is associated with decreased deposition of extracellular matrix and reduced tumor cell apoptosis., Mol. Cancer Res. 2 (2004) 215–24. http://www.ncbi.nlm.nih.gov/pubmed/15140943 (accessed December 3, 2019).

[38] S. Arnold, E. Mira, S. Muneer, G. Korpanty, A.W. Beck, S.E. Holloway, S. Mañes, R.A. Brekken, Forced expression of MMP9 rescues the loss of angiogenesis and abrogates metastasis of pancreatic tumors triggered by the absence of host SPARC, Exp. Biol. Med. 233 (2008) 860–873. https://doi.org/10.3181/0801-RM-12.

[39] S.A. Arnold, L.B. Rivera, J.G. Carbon, J.E. Toombs, C.L. Chang, A.D. Bradshaw, R.A. Brekken, Losartan slows pancreatic tumor progression and extends survival of SPARC-null mice by abrogating aberrant TGFβ activation, PLoS One. 7 (2012). https://doi.org/10.1371/journal.pone.0031384.

[40] S.A. Arnold, R.A. Brekken, SPARC: A matricellular regulator of tumorigenesis, J. Cell Commun. Signal. 3 (2009) 255–273. https://doi.org/10.1007/s12079-009-0072-4.

[41] S.A. Arnold, L.B. Rivera, A.F. Miller, J.G. Carbon, S.P. Dineen, Y. Xie, D.H. Castrillon, E.H. Sage, P. Puolakkainen, A.D. Bradshaw, R.A. Brekken, Lack of host SPARC enhances vascular function and tumor spread in an orthotopic murine model of pancreatic carcinoma, DMM Dis. Model. Mech. 3 (2010) 57–72. https://doi.org/10.1242/dmm.003228.

[42] K.Y. Aguilera, L.B. Rivera, H. Hur, J.G. Carbon, J.E. Toombs, C.D. Goldstein, M.T. Dellinger, D.H. Castrillon, R.A. Brekken, Collagen signaling enhances tumor progression after anti-VEGF therapy in a murine model of pancreatic ductal adenocarcinoma, Cancer Res. 74 (2014) 1032–1044. https://doi.org/10.1158/0008-5472.CAN-13-2800.

[43] I. Ramu, S.M. Buchholz, M.S. Patzak, R.G. Goetze, S.K. Singh, F.M. Richards, D.I. Jodrell, B. Sipos, P. Ströbel, V. Ellenrieder, E. Hessmann, A. Neesse, SPARC dependent collagen deposition and gemcitabine delivery in a genetically engineered mouse model of pancreas cancer, EBioMedicine. 48 (2019) 161–168. https://doi.org/10.1016/j.ebiom.2019.09.024.

[44] M. Rahman, A.P.K. Chan, I.T. Tai, A peptide of sparc interferes with the interaction between Caspase8 and Bcl2 to resensitize Chemoresistant tumors and enhance their regression in vivo, PLoS One. 6 (2011). https://doi.org/10.1371/journal.pone.0026390.

[45] P. Hasselaar, E.H. Sage, SPARC antagonizes the effect of basic fibroblast growth factor on the migration of bovine aortic endothelial cells, J. Cell. Biochem. 49 (1992) 272–283. https://doi.org/10.1002/jcb.240490310.

[46] S. V. Vadlamuri, J. Media, S.S. Sankey, A. Nakeff, G. Divine, S.A. Rempel, SPARC affects glioma cell growth differently when grown on brain ECM proteins in vitro under standard versus reduced-serum stress conditions, Neuro. Oncol. 5 (2003) 244–254. https://doi.org/10.1093/neuonc/5.4.244.

[47] N.F. Li, E. Gemenetzidis, F.J. Marshall, D. Davies, Y. Yu, K. Frese, F.E.M. Froeling, A.K. Woolf, R.M. Feakins, Y. Naito, C. Iacobuzio-Donahue, D.A. Tuveson, I.R. Hart, H.M. Kocher, RhoC interacts with integrin α5β1 and enhances its trafficking in migrating pancreatic carcinoma cells, PLoS One. 8 (2013). https://doi.org/10.1371/journal.pone.0081575.

[48] T.H. Barker, G. Baneyx, M. Cardó-Vila, G.A. Workman, M. Weaver, P.M. Menon, S. Dedhar, S.A. Rempel, W. Arap, R. Pasqualini, V. Vogel, E.H. Sage, SPARC regulates extracellular matrix organization through its modulation of integrin-linked kinase activity, J. Biol. Chem. 280 (2005) 36483–36493. https://doi.org/10.1074/jbc.M504663200.

[49] J. Nie, E. Helene Sage, SPARC inhibits adipogenesis By its enhancement of β-catenin signaling, J. Biol. Chem. 284 (2009) 1279–1290. https://doi.org/10.1074/jbc.M808285200.

Figure legends.

Figure 1: Validation of SPARC knockdown (KD) in stromal PS-1 cells. (**A**) Western blot representative of 3 independent experiments showing SPARC expression in pancreatic cancer and stromal (PS-1) cells. (**B**) PS-1 cells were treated with the indicated concentration of control- or SPARC (#J-003710-10)-siRNA, and western blot of SPARC expression (42kDa) is shown (n=1). (**C**) Graph shows percentage SPARC KD in transfection experiments in this study (80nM siRNA); dotted line shows mean KD. (**D**) Representative western blot shows SPARC KD using 80nM #J-003710-10 siRNA. (**E**) Western blot showing SPARC knockdown using an alternative SPARC siRNA (#J-003710-09). **(F)** SPARC secretion in conditioned media from PS-1 cells treated with control- or SPARC siRNA, as determined by ELISA assay. Graph shows mean SPARC (ng/ml) +/- SEM (n=3).

Figure 2: Stroma-derived SPARC promotes pancreatic cancer cell proliferation *in vitro*. (**A**) pancreatic cancer cells were treated with conditioned medium from control- or SPARC-siRNA transfected PS-1 cells (10% FBS). Cell proliferation was measured by BrdU assay for the last 24hrs of 72hr culture. Graph shows relative absorbance ±SEM (n=24-60 from 3-4 independent experiments). (**B&C**) AsPC-1 cells were co-cultured with PS-1 cells previously transfected with either control- or SPARC-siRNA (10%FBS) in a transwell model using a 1µm porous insert, and cancer cell density was determined by haemocytometre counting. (**B**) Graph shows mean AsPC-1 cell density over 5 consecutive days ± SEM (n=4 from 4 independent experiments). (**C**) Graph shows mean relative AsPC-1 cell density at day 6 (n=9 from 3 independent experiments), and representative images are also shown.

Figure 3: No evidence for autocrine effect of SPARC on pancreatic stellate cells. (**A**) graph shows mean relative PS-1 cell density ±SEM at 48 hours following siRNA transfection in a 24 well plate as determined by haemocytometer cell counting (n=18 from 4 independent experiments)**.** (**B**) Following control-/SPARC-siRNA transfection, PS-1 cells were re-plated in their own conditioned medium in a 96 well plate and proliferation was determined by BrdU assay. Graph shows mean absorbance ±SEM (n=12 from 2 independent experiments). (**C**), PS-1 cells were treated +/- 10µg/ml rhSPARC and BrdU incorporation was measured for the last 24hrs of 72hr culture (n=18-36 from 3-6 independent experiments. (**D**) Representative western blot and table show vimentin expression in transfected PS-1 cells (n=6 from 6 independent experiments). **(E)** Vimentin expression in transfected PS-1 cells grown in complete medium on coverslips in a 6 well plate was also determined by quantitative microscopy using ImageJ software. Representative images of vimentin expression are shown in (**E**), where the scale bar represents 200µm (taken with 10X objective), and quantitative data is shown in (**F**), where the graph shows relative intensity of vimentin (n=9 from 3 independent experiments). Cell

density was also determined from these images, and mean cell density +/-SEM is shown in (**G**). Representative western blot in (**H**) shows TGF-β expression in PS-1 cells cultured for 3 consecutive days after re-plating following transfection with SPARC or control siRNA. Graph in (**I**) shows mean TGF-β expression relative to day 0 control. Data pooled from 3 independent experiments (n=3). All experiments performed in complete media (10% FBS).

Figure 4: Purified SPARC mimics the effect of PS-1-derived SPARC. (**A**&**B**), rhSPARC and PS-1-derived SPARC were treated with PNGaseF to remove N-linked glycosylation and analysed by western blot. Representative blots are shown in (**A**)**,** and in (**B**) the mean molecular weight of rhSPARC and PS-1 SPARC pre- and post-deglycosylation from 5 independent experiments is shown, determined using Image Studio Lite V. 4.0 software. In (**C**), pancreatic cancer cells were treated with 10μg/ml rhSPARC in complete medium (10% FBS), n=18-30 from 3-5 independent experiments.

Figure 5: Fibronectin controls proliferative SPARC function. (**A**) Pancreatic cancer cells were cultured in low serum (0.5% FBS) conditioned medium collected from control- or SPARC-siRNA transfected PS-1 cells (n=24-60 from 3-4 independent experiments). (**B**) AsPC-1 and Hpaf cells were cultured in conditioned medium (10% or 0.5% FBS) from PS-1 cells transfected with control- or SPARC-siRNA. A different SPARC siRNA was used for this experiment, targeting a distinct sequence from that used in earlier experiments (see methods for details; validation of knockdown is shown in Figure 1E). Graph shows relative absorbance ±SEM (n= 24 from 4 independent experiments). (**C**) AsPC-1 cells were cultured in medium containing 10% FBS, 0.25% BSA (0% FBS) and 0% FBS and treated +/- 10μg/ml rhSPARC (n=12 from 2 independent experiments). (**D**), AsPC-1 cells were cultured in low serum medium (0.5% FBS) and treated with 10μg/ml rhSPARC, 140ng/ml TGF-β or both rhSPARC & TGF-β (n=17-18 from 3 independent experiments). Statistical significance was determined by two-way ANOVA. (**E**), AsPC-1 cells were cultured in low serum medium (0.5% FBS), complete medium (10% FBS) or complete medium depleted of fibronectin (10% FBS - FN), and treated +/- 10μg/ml rhSPARC (n=18 from 3 independent experiments). (**F**&**G**) AsPC-1 cells were cultured in 0.5% FBS +/- 10μg/ml rhSPARC SPARC and +/- fibronectin at either 500 μg/ml (F) or 1 mg/ml (G). In (**A**-**G**)**,** proliferation was measured by BrdU assay for the last 24hrs of a 72hr culture, and graphs show mean relative absorbance ±SEM.

Figure 6: Fibronectin switches SPARC activity from promoting cell growth to induction of apoptosis. (**A-C**), Hpaf cells were treated +/- 10 μg/ml rhSPARC and cultured for 72hrs, in either low serum (**A**), or normal 10% serum (**B**), conditions, and as indicated in (**C**). Detection of caspase-3/7 activity was quantified every 24hrs over a 72 hour period using an Incucyte Zoom live cell imaging system (Essen Bioscience). Graphs in (**A**&**B**) shown mean fluorescent area +/- SEM, representing caspase-3/7 activity. (**C**) Representative images at 72hrs are shown (n=18 from 3 independent experiments). Similar results were seen with AsPC-1 cells (data not shown). (**D**&**E**) AsPC-1 cells were cultured in 10% FBS medium depleted of fibronectin and treated +/- SPARC for 72 hours (n=3). (**D**) cell number was determined by haemocytometer counting. (**E**) Early stage apoptosis was measured using flow cytometry to quantify Annexin V binding. Cells were gated on the live ($7AAD^-$) population.

Figure 1

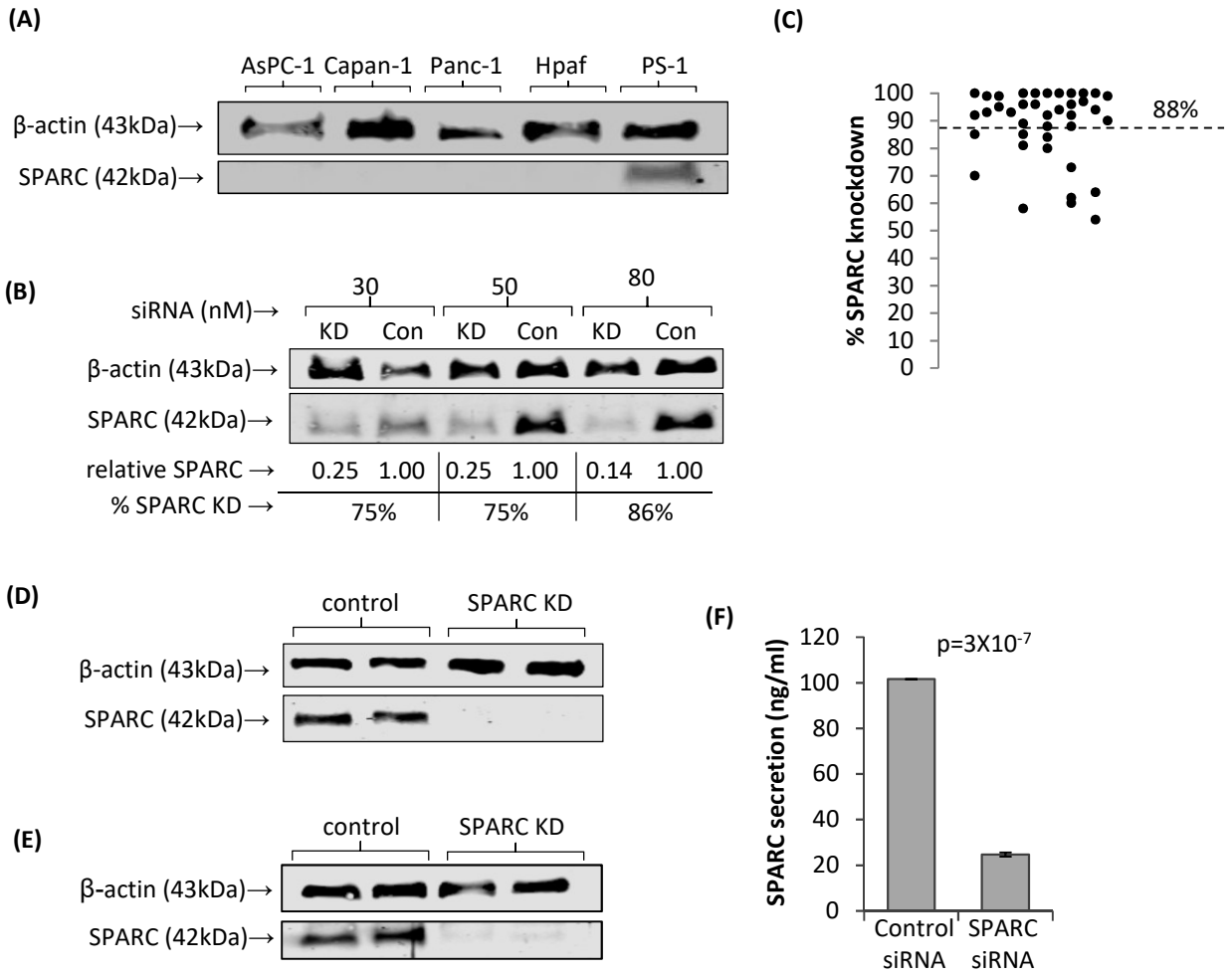
(A)
AsPC-1
Capan-1
Panc-1
Hpaf
PS-1
β-actin (43kDa)→
SPARC (42kDa)→
(B)
siRNA (nM)→
30
50
80
KD
Con
KD
Con
KD
Con
β-actin (43kDa)→
SPARC (42kDa)→
relative SPARC →
0.25
1.00
0.25
1.00
0.14
1.00
% SPARC KD →
75%
75%
86%
(C)
% SPARC knockdown
100
90
80
70
60
50
40
30
20
10
0
88%
(D)
control
SPARC KD
β-actin (43kDa)→
SPARC (42kDa)→
(E)
control
SPARC KD
β-actin (43kDa)→
SPARC (42kDa)→
(F)
SPARC secretion (ng/ml)
120
100
80
60
40
20
0
p=3X10-7
Control siRNA
SPARC siRNA

Figure 2

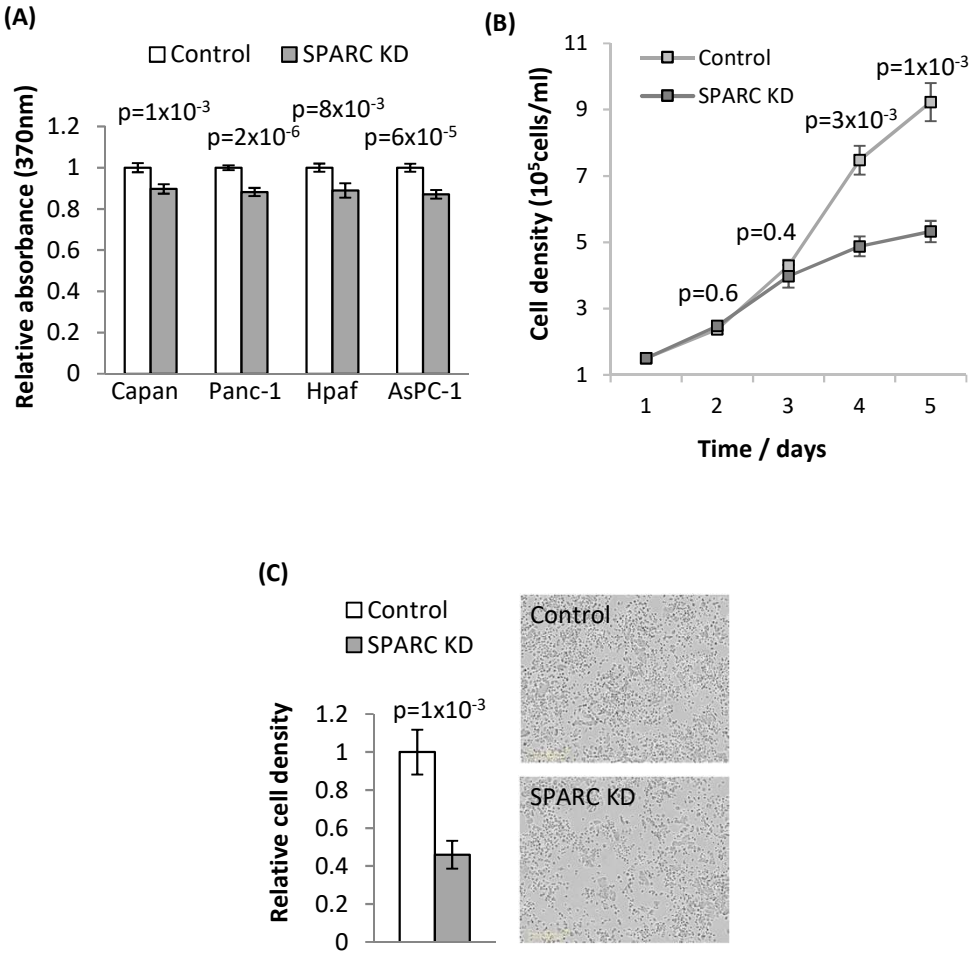
(A)
Control
SPARC KD
p=1x10-3
p=2x10-6
p=8x10-3
p=6x10-5
Relative absorbance (370nm)
1.2
1
0.8
0.6
0.4
0.2
0
Capan
Panc-1
Hpaf
AsPC-1
(B)
Control
SPARC KD
p=1x10-3
p=3x10-3
p=0.4
p=0.6
Cell density (10^5cells/ml)
11
9
7
5
3
1
1
2
3
4
5
Time / days
(C)
Control
SPARC KD
p=1x10-3
Relative cell density
1.2
1
0.8
0.6
0.4
0.2
0
Control
SPARC KD

Figure 3

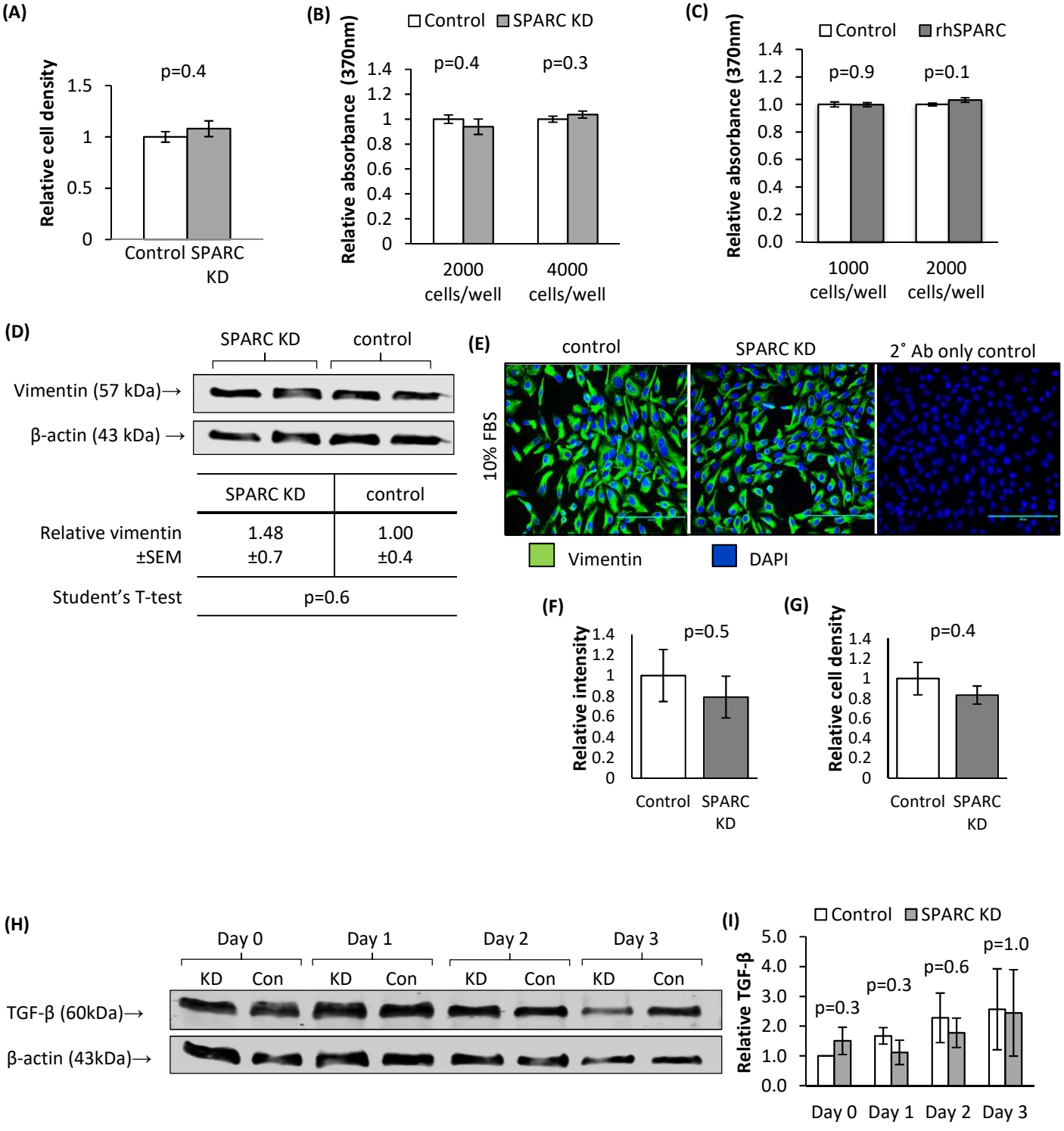
(A)
Relative cell density
p=0.4
Control
SPARC KD
(B)
Control
SPARC KD
Relative absorbance (370nm)
p=0.4
p=0.3
2000 cells/well
4000 cells/well
(C)
Control
rhSPARC
Relative absorbance (370nm)
p=0.9
p=0.1
1000 cells/well
2000 cells/well
(D)
SPARC KD
control
Vimentin (57 kDa)→
β-actin (43 kDa) →
SPARC KD
control
Relative vimentin ±SEM
1.48 ±0.7
1.00 ±0.4
Student's T-test
p=0.6
(E)
control
SPARC KD
2˚ Ab only control
10% FBS
Vimentin
DAPI
(F)
Relative intensity
p=0.5
Control
SPARC KD
(G)
Relative cell density
p=0.4
Control
SPARC KD
(H)
Day 0
Day 1
Day 2
Day 3
KD
Con
TGF-β (60kDa)→
β-actin (43kDa)→
(I)
Control
SPARC KD
Relative TGF-β
p=0.3
p=0.3
p=0.6
p=1.0
Day 0
Day 1
Day 2
Day 3

Figure 4

(A)

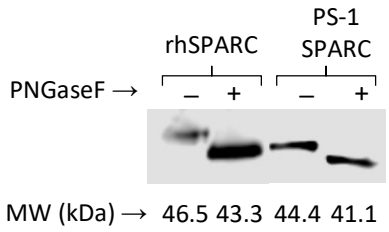

(B)

	rhSPARC		PS-1 SPARC	
PNGase F	-	+	-	+
MW (kDa) ±SEM	47.2 ±0.9	44.1 ±1.1	44.1 ±1.5	41.5 ±0.5
Shift (kDa)	3.1		2.6	
T-test	P=0.01		P=0.1	

(C)

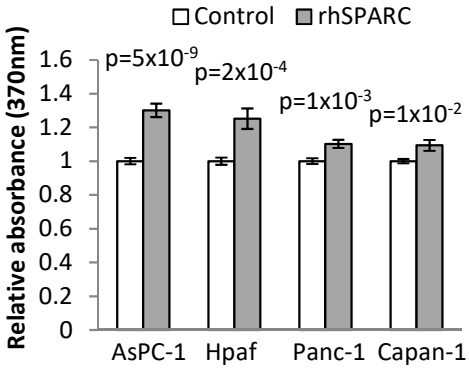

Figure 5

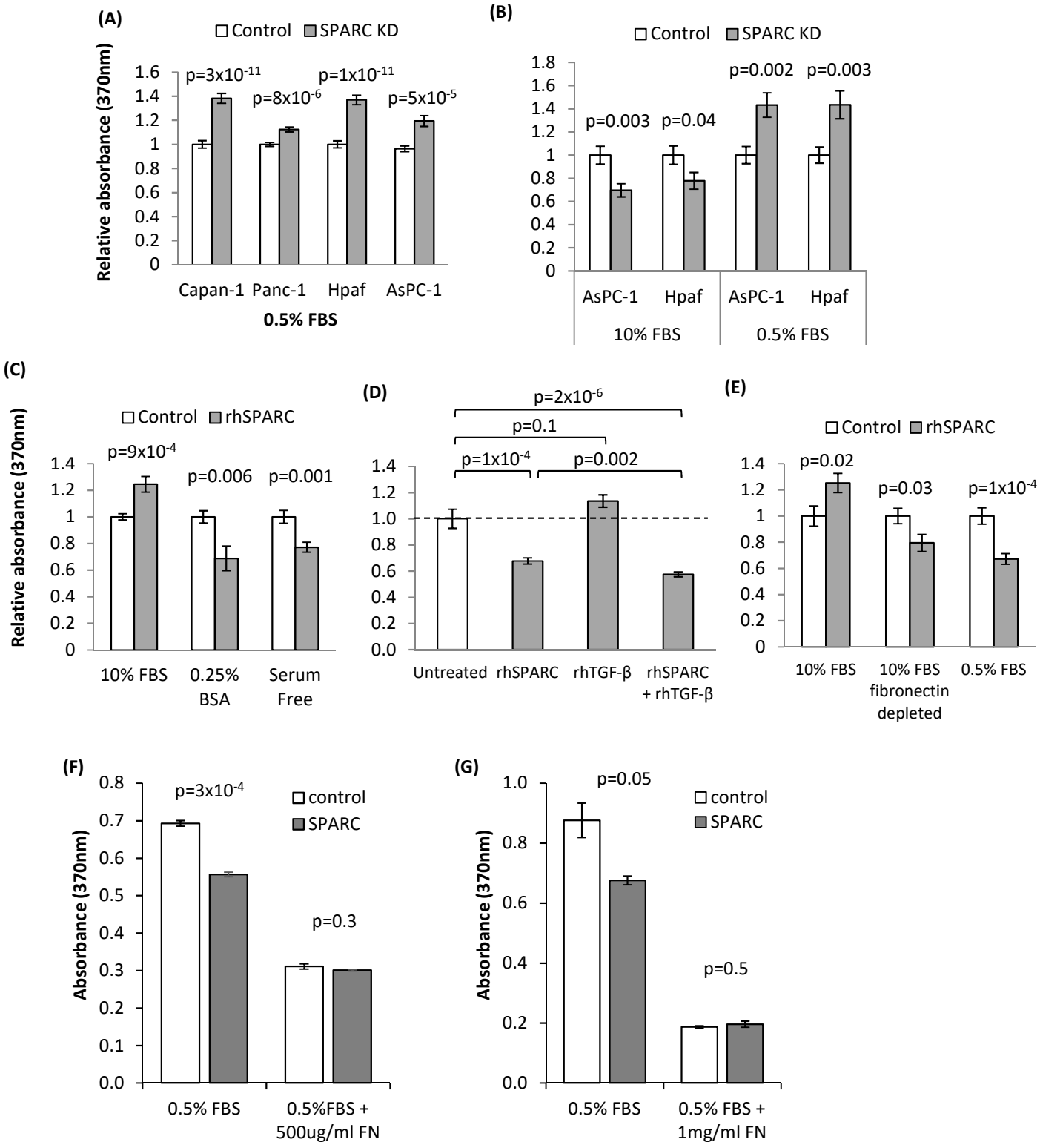
(A)
Control
SPARC KD
Relative absorbance (370nm)
p=3x10-11
p=8x10-6
p=1x10-11
p=5x10-5
Capan-1
Panc-1
Hpaf
AsPC-1
0.5% FBS
(B)
Control
SPARC KD
p=0.003
p=0.04
p=0.002
p=0.003
AsPC-1
Hpaf
AsPC-1
Hpaf
10% FBS
0.5% FBS
(C)
Control
rhSPARC
Relative absorbance (370nm)
p=9x10-4
p=0.006
p=0.001
10% FBS
0.25% BSA
Serum Free
(D)
p=2x10-6
p=0.1
p=1x10-4
p=0.002
Untreated
rhSPARC
rhTGF-β
rhSPARC + rhTGF-β
(E)
Control
rhSPARC
p=0.02
p=0.03
p=1x10-4
10% FBS
10% FBS fibronectin depleted
0.5% FBS
(F)
control
SPARC
Absorbance (370nm)
p=3x10-4
p=0.3
0.5% FBS
0.5%FBS + 500ug/ml FN
(G)
control
SPARC
Absorbance (370nm)
p=0.05
p=0.5
0.5% FBS
0.5% FBS + 1mg/ml FN

Figure 6

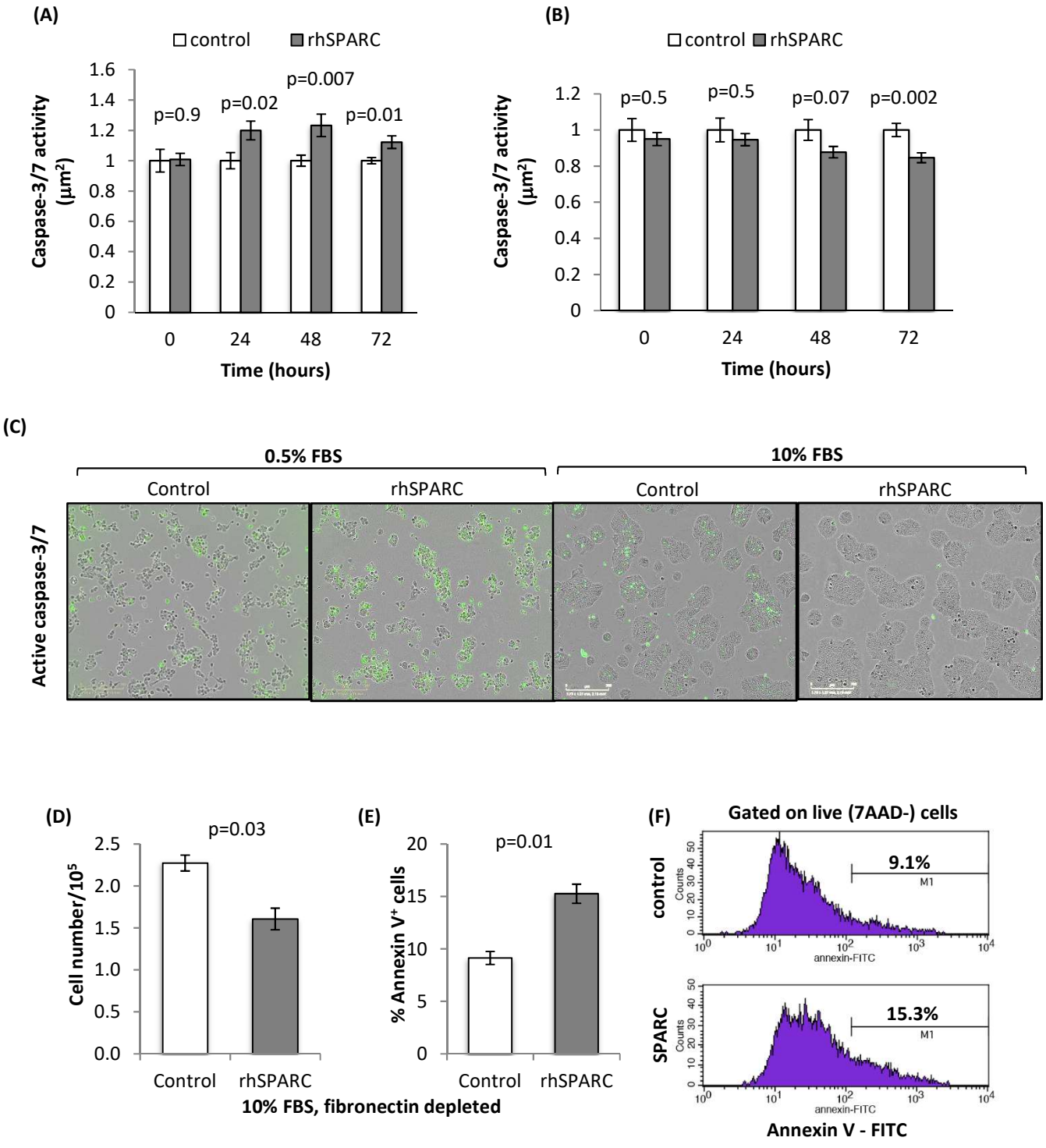
(A)
control
rhSPARC
Caspase-3/7 activity (µm²)
p=0.9
p=0.02
p=0.007
p=0.01
Time (hours)
(B)
control
rhSPARC
Caspase-3/7 activity (µm²)
p=0.5
p=0.5
p=0.07
p=0.002
Time (hours)
(C)
0.5% FBS
10% FBS
Control
rhSPARC
Control
rhSPARC
Active caspase-3/7
(D)
p=0.03
Cell number/10⁵
Control
rhSPARC
(E)
p=0.01
% Annexin V⁺ cells
Control
rhSPARC
10% FBS, fibronectin depleted
(F)
Gated on live (7AAD-) cells
control
9.1%
M1
Counts
annexin-FITC
SPARC
15.3%
M1
Counts
annexin-FITC
Annexin V - FITC

Supplementary Figure 1

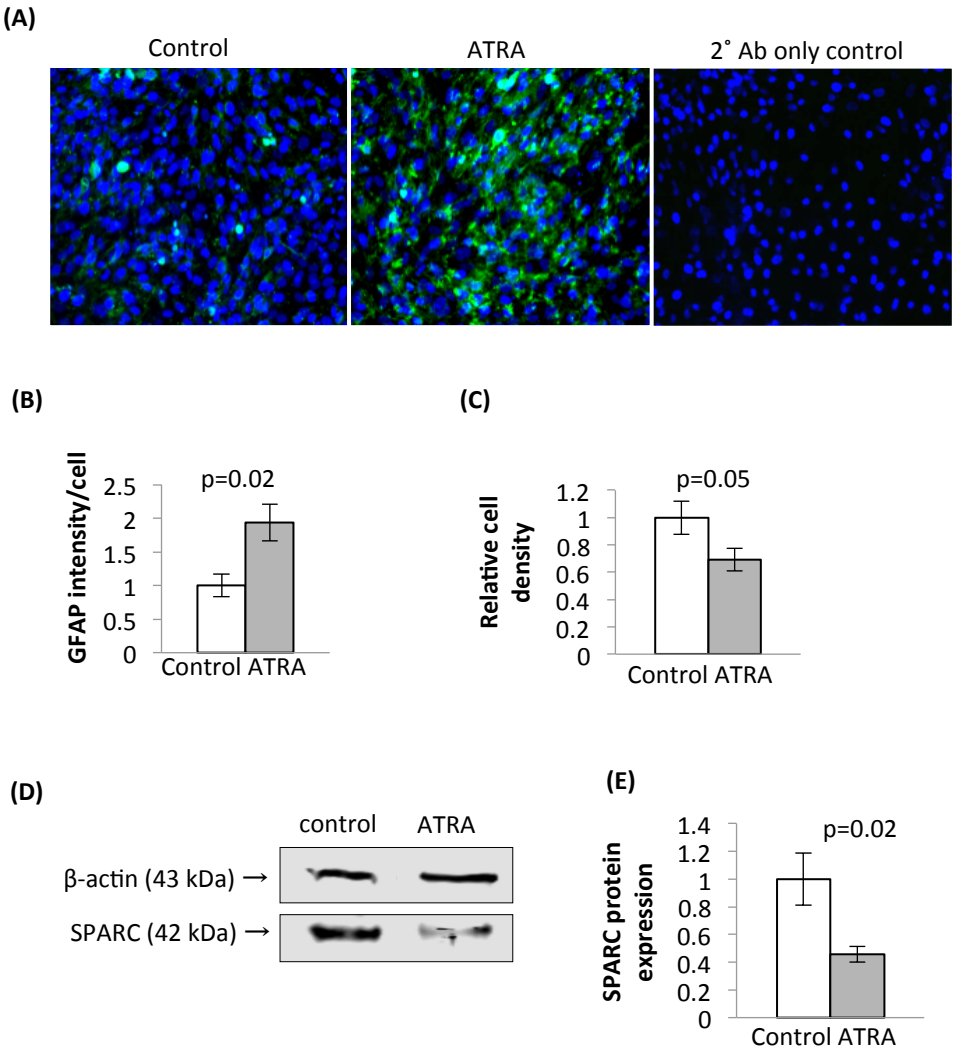

Supplementary Figure 2

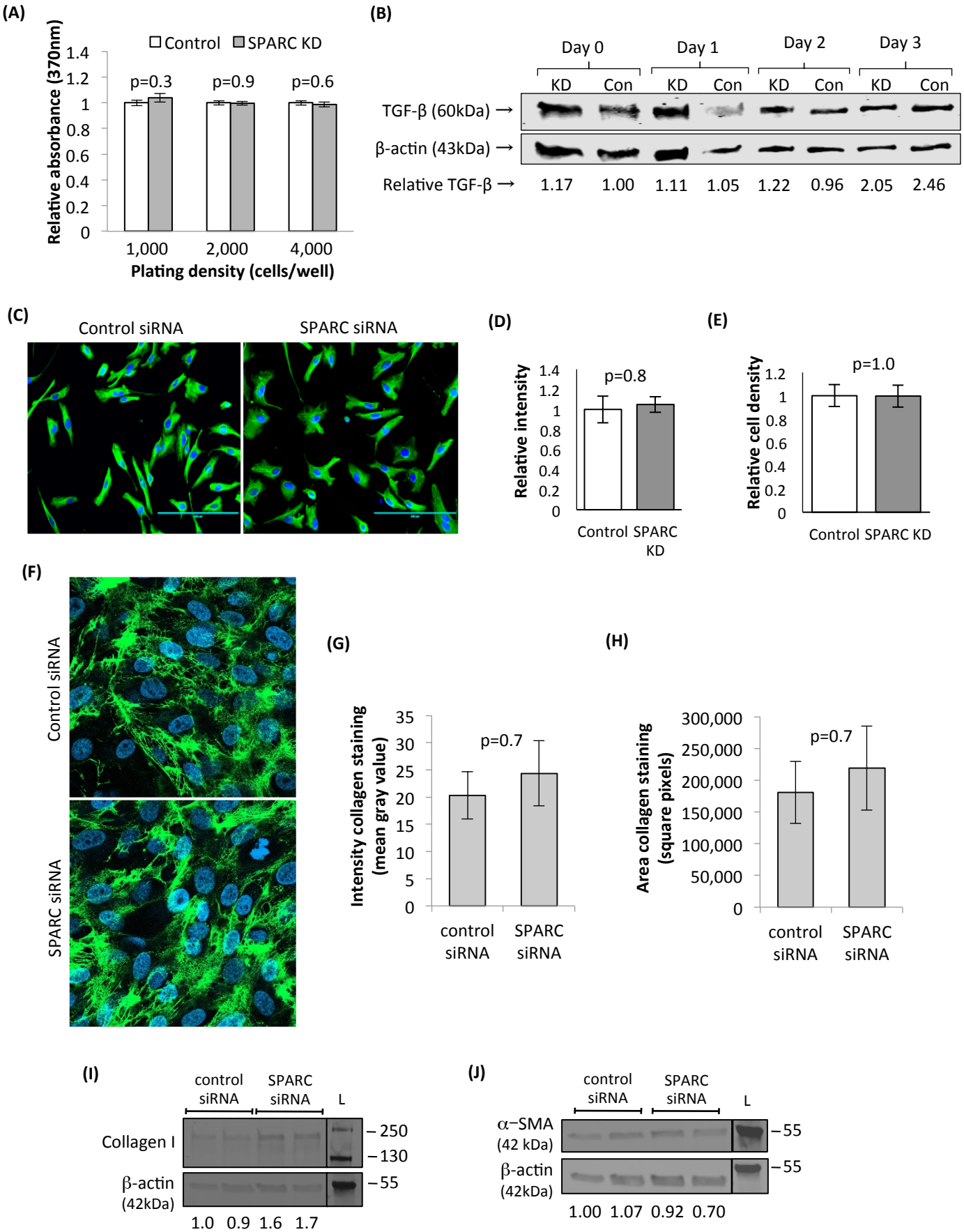

Supplementary Figure 3

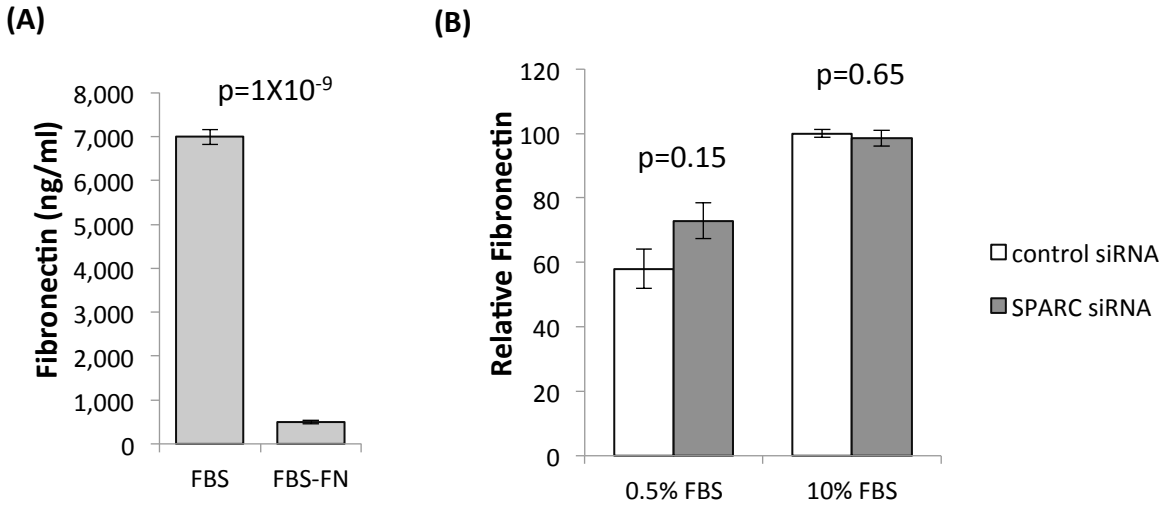

Supplementary Table 1: Details of antibodies used in this study.

Application	Antibody	Manufacturer	Catalogue number	Dilution*
Immunocytochemistry (ICC)	Anti-rabbit Alexafluor488	Life Technologies	A-11001	1:200
	Anti-goat Alexafluor488	Life Technologies	A-11055	1:200
	Anti-goat collagen I polyclonal	Abcam	ab19811	1:100
	Anti-mouse GFAP monoclonal	Sigma-Aldrich	G3893	1:50
	Anti-mouse vimentin (V9) monoclonal	Dako	MO725	1:200
Western blot (WB)	Anti-mouse β-actin monoclonal	Abcam	ab8224	1:5,000
	Anti-rabbit collagen I polyclonal	Abcam	ab34710	1:2,500
	Anti-mouse α-SMA monoclonal	Abcam	ab7817	1:300
	Anti-rabbit SPARC (H-90) polyclonal	Santa Cruz Biotechnology	sc-25574	1:1,000
	Anti-rabbit TGF-β polyclonal	Abcam	ab66043	1:5,000
	Anti-mouse vimentin (V9) monoclonal	Dako	MO725	1:2,500
	Anti-mouse IRDye 680RD	Li-Cor	926-68070	1:10,000
	Anti-rabbit IRDye 800CW	Li-Cor	926-32211	1:10,000

*All ICC antibodies were diluted in PBS and WB antibodies in TTBS

Supplementary Table 2: Serum components and potential SPARC binding partners.

Protein	Predicted to interact with SPARC		Evidence for presence in serum	References
	NCBI Gene database	STRING database		
Albumin		Yes	Yes	S1
Cathepsin K	Yes		Yes	S2
Collagen type I α1-chain	Yes	Yes	No	
Collagen type I α2-chain	Yes	Yes	No	
Collagen type II α1-chain	Yes		No	
Collagen type III α1-chain	Yes		No	
Collagen type V α1-chain	Yes		No	
Collagen type XIII α1-chain	Yes		No	
Cytoplasmic polyadenylation element binding protein 2	Yes		No	
Fibronectin 1	Yes	Yes	Yes	S1
Heparan sulphate proteoglycan 2	Yes		No	
Plasminogen	Yes	Yes	Yes	S3
Plasminogen activator, tissue type	Yes		No*	
Platelet derived growth factor-α	Yes		Yes	S1
Platelet derived growth factor-β		Yes	Yes	S1
Ras association domain family member 7	Yes		No	
Syndecan 2	Yes		No	
Thrombospondin 1	Yes	Yes	Yes	S4
TIMP metallopeptidase inhibitor 1		Yes	Yes	S5
Transforming growth factor β1	Yes	Yes	Yes	S1
Transglutaminase 2	Yes		No*	
Ubiquilin 1	Yes		No	
Vasoendothelial growth factor A	Yes	Yes	Yes	S6
X-ray repair cross complementing 6	Yes		No	
Zinc finger protein 579	Yes		No	

*can be secreted under certain conditions
NCBI gene database, U.S. National Library of Medicine: https://www.ncbi.nlm.nih.gov/gene [last accessed: 05/07/19]
STRING database, STRING consortium 2019: https://string-db.org/ [last accessed: 05/07/19]
Proteins in grey are predicted to interact with SPARC and are likely to be present in serum.

Supplementary figure legends

Supplementary figure 1: SPARC expression is higher in activated compared to quiescent PS1 cells. PS1 cells were treated for 7 days with 1μM ATRA. (**A**) Representative ICC images are shown of GFAP staining in control and ATRA treated PS-1 cells. (**B**) Quantitative analysis of relative GFAP intensity per cell and (**C**) relative cell density are also shown (n=7-9 from 3 independent experiments). SPARC expression was quantified by Western blot, and representative images (**D**) and quantitative analysis (**E**) are shown (n=6 from 3 independent experiments).

Supplementary figure 2: SPARC does not affect PS-1 proliferation or activation under low serum conditions. (**A**) PS-1 cells were transfected for 48hrs with or control- or SPARC-siRNA in low serum medium (0.5% FBS). Post transfection, PS-1 cells were re-plated into a 96 well plate in their own conditioned media and BrdU incorporation was measured for the last 24hrs of 72hr culture (n=20-40 from 2-3 independent experiments). (**B**) TGF-β expression was determined by western blot in re-plated control-/SPARC-siRNA transfected PS-1 cells in low serum medium (0.5% FBS). A representative blot from two independent experiments is shown. Numbers under the blot indicate TGF-β band intensity standardised to β-actin loading control. (**C-D**) Vimentin expression in transfected PS-1 cells cultured in low serum medium (0.5% FBS) on coverslips in a 6 well plate was determined by quantitative microscopy using ImageJ software. Representative images of vimentin expression are shown in (**C**), where the scale bar represents 200μm (taken with 10x objective), and quantitative data is shown in (**D**), where the graph shows relative intensity of vimentin (n=9 from 3 independent experiments). (**E**) Cell density was also determined from these images, and mean cell density +/-SEM is shown. (**F-H**) Collagen staining of non-permeabilised control- and SPARC-siRNA treated PS1 cells was imaged using confocal microscopy. Representative images are shown in **(F)**, with quantification of staining intensity (**G**) and area (**H**) also shown (n=3, with 3-4 images quantified per slide). Secondary only control staining for both collagen and vimentin was blank. (**I&J**) Cell lysates from control- and SPARC-siRNA treated cells were analysed by western blot for expression of collagen I (**I**) and α-SMA (**J**). 'L' indicates size marker/ladder. Quantification of band intensity is shown under each blot, standardised to β-actin loading control and relative to the first lane.

Supplementary figure 3: Fibronectin quantification. ELISA was used to measure fibronectin concentration (**A**) in FBS samples before and after fibronectin depletion using gelatin-sepharose depletion (n=3), and (**B**) in media from PS-1 cells following treatment with either control- or SPARC-siRNA, in 0.5% and 10% serum as indicated (n=6 from two independent experiments).

Supplementary References.

[1] D. Brunner, J. Frank, H. Appl, H. Schöffl, W. Pfaller, G. Gstraunthaler, Serum-free cell culture: the serum-free media interactive online database., ALTEX. 27 (2010) 53–62. https://doi.org/10.14573/altex.2010.1.53.

[2] C. Meier, U. Meinhardt, J.R. Greenfield, J. De Winter, T. V. Nguyen, C.R. Dunstan, M.J. Seibel, Serum cathepsin K concentrations reflect osteoclastic activity in women with postmenopausal osteoporosis and patients with Paget's disease, Clin. Lab. 52 (2006) 1–10. http://www.ncbi.nlm.nih.gov/pubmed/16506358 (accessed December 20, 2019).

[3] S.A. Cederholm-Williams, Concentration of plasminogen and antiplasmin in plasma and serum, J. Clin. Pathol. 34 (1981) 979–981. https://doi.org/10.1136/jcp.34.9.979.

[4] C. Jenkinson, V.L. Elliott, A. Evans, L. Oldfield, R.E. Jenkins, D.P. O'brien, S. Apostolidou, A. Gentry-Maharaj, E.O. Fourkala, I.J. Jacobs, U. Menon, T. Cox, F. Campbell, S.P. Pereira, D.A.

Tuveson, B.K. Park, W. Greenhalf, R. Sutton, J.F. Timms, J.P. Neoptolemos, E. Costello, Decreased serum thrombospondin-1 levels in pancreatic cancer patients up to 24 months prior to clinical diagnosis: Association with diabetes mellitus, Clin. Cancer Res. 22 (2016) 1734–1743. https://doi.org/10.1158/1078-0432.CCR-15-0879.

[5] M. Kozłowski, W. Laudański, B. Mroczko, M. Szmitkowski, R. Milewski, G. Łapuć, Serum tissue inhibitor of metalloproteinase 1 (TIMP-1) and vascular endothelial growth factor A (VEGF-A) are associated with prognosis in esophageal cancer patients, Adv. Med. Sci. 58 (2013) 227–234. https://doi.org/10.2478/ams-2013-0017.

[6] A. Larsson, E. Sköldenberg, H. Ericson, Serum and plasma levels of FGF-2 and VEGF in healthy blood donors, Angiogenesis. 5 (2002) 107–110. https://doi.org/10.1023/A:1021588227705.